


Post-mortem analysis of a commercial Copper Indium Gallium Diselenide (CIGS) photovoltaic module after potential induced degradation

Pelin Yilmaz^{1,2}  | Rémi Aninat² | Gonzalo Ott Cruz² | Thomas Weber³ | Jurriaan Schmitz¹ | Mirjam Theelen²

¹MESA+ Institute for Nanotechnology, University of Twente, Enschede, The Netherlands

²TNO partner in Solliance, Eindhoven, The Netherlands

³PI Photovoltaik-Institut Berlin AG, Berlin, Germany

Correspondence

Pelin Yilmaz, MESA+ Institute for Nanotechnology, University of Twente, Enschede, The Netherlands.
Email: p.yilmaz@utwente.nl

Funding information

Early Research Program 'Sustainability & Reliability for solar and other (opto-)electronic thin-film devices' (STAR) from TNO

Abstract

An extensive post-mortem analysis was conducted on a commercial copper-(indium-gallium)-diselenide (CIGS) photovoltaic module that degraded after exposure to the high voltage stress of a standardized potential induced degradation (PID) test. We employed a custom-developed *coring* technique to extract samples from the full-size field module, which showed degraded and nondegraded areas (regarded as reference) in electroluminescence after the PID test. The resulting solar cell samples were compared based on their electrical properties and sodium profiles using a wide range of laboratory-based analysis techniques including photoluminescence and lock-in thermography imaging, current–voltage measurements, and glow discharge optical emission spectroscopy. The samples that were extracted from the degraded areas of the module showed lower photoluminescence intensity and had significantly lower open-circuit voltage V_{oc} and fill factor (FF) values in comparison with reference samples. An increased content of sodium within the absorber layer was also observed for these samples, linking sodium migration to PID. These observations at the module level are consistent with earlier reports on PID-stressed CIGS cells and mini-modules. This is to our knowledge the first reported study of a microscopic investigation on a real-life full-scale CIGS module after PID.

KEYWORDS

CIGS, coring, post-mortem analysis, potential-induced degradation, reliability, thin film photovoltaics

1 | INTRODUCTION

Considering the large investment and increasing dependence on photovoltaic (PV) modules, their reliability has become an important topic of interest issue in the PV community. PV modules in the field can degrade over time through various wear-out mechanisms, reducing their power production and limiting the module lifetime.^{1,2} One

common degradation mechanism is potential induced degradation (PID), particularly observed in larger PV modules. In such installations, many PV modules are connected in series to maximise the system voltage, currently reaching up to 1500 V (positive or negative) in some PV power plants, and grounding is applied for safety purposes.³ PID originates from the high potential difference between the solar cells on one hand and the grounded frame and/or mounting rails on the

This is an open access article under the terms of the Creative Commons Attribution License, which permits use, distribution and reproduction in any medium, provided the original work is properly cited.

© 2022 The Authors. Progress in Photovoltaics: Research and Applications published by John Wiley & Sons Ltd.

other. The potential difference leads to leakage current formation that can take various pathways across and through the module.⁴ It can also induce sodium migration which is abundant in the glass sheets. Efficiency and power losses have been linked to this sodium migration from the glass to the solar cell.⁵ Sodium accumulation within the solar cell affects its electrical properties.

The PID phenomenon can be observed in all PV technologies. Copper-(indium-gallium)-diselenide (CIGS) PV modules have demonstrated higher resistance against PID in comparison with multicrystalline Si and a-Si, when mini-modules of each type were compared under the same testing conditions.⁶ Severe PID failures in the field have only been reported for a specific CIGS manufacturer. However, considering the current objectives to increase the maximum system voltages to even higher values than ± 1500 V, the degradation risks due to PID may also rise for CIGS PV modules. It is therefore important to study and understand the degradation mechanisms behind PID. The underlying mechanisms for PID largely differ for each technology; the mechanisms of shunting at stacking faults and the surface polarisation effect that are common in c-Si PV modules are not observed in CIGS modules.^{7,8} For CIGS PV modules, p-n junction damage or transparent conductive oxide (TCO) corrosion due to sodium accumulation are proposed as root causes of the degradation.^{6,9-11} However, contradictory results have been reported. We have recently published a review article that presents an overview of the published studies of PID in CIGS PVs including reported field observations, testing methods, observations of sodium migration and leakage current, degradation mechanisms, and mitigation approaches.¹² As presented by the review article, a full understanding of PID is yet to be achieved.

One reason for incomplete understanding of PID is the lack of comparisons and poor correlations, particularly between field and laboratory studies. This is because of differences in test setups and test parameters in reported studies, in addition to varying module and cell design. The extend of analysis after PID testing also varies. For example, field studies focus mainly on macroscopic investigations such as tracking of the electrical properties upon PID stressing.^{4,13} Due to the packaging of the field modules with glass sheets and encapsulant, such studies can only report current-voltage and leakage current measurements, which yields limited information on the nature of the defects and the root causes of PID.

On the other hand, in-depth microanalyses have only been possible with laboratory-made CIGS devices.^{11,14-16} Sodium migration and accumulation within the different layers of CIGS solar cell have been reported, which helps to identify degradation mechanisms behind PID.^{9,16,17} However, such studies were carried out on cells or mini-modules without the full encapsulation stack; therefore, the samples, as well as the exposure conditions, may not be representative of field modules. This creates a gap between the two areas of expertise and makes it difficult to correlate the studies and observations to reach common conclusions on PID.

In this study, we aim to bridge this gap by conducting a post-mortem analysis at the microscopic scale via laboratory-based techniques on a commercial frameless CIGS field module that was PID tested following the IEC 62804-1 standard. The module was selected from a specific early production batch of a commercial supplier (2010) that exhibited enhanced PID in the field. Areas of interest for post-mortem analysis, including both degraded and nondegraded areas of the full-size module, were defined based on the electroluminescence (EL) image of the module after the PID test. From these areas of interest, representative samples were extracted by coring and then unpackaged for an extensive post-mortem analysis. The analysis includes photoluminescence (PL) and illuminated lock-in thermography (ILIT) imaging, current-voltage (I-V) measurements, and glow discharge optical emission spectroscopy (GD-OES).

2 | EXPERIMENTAL METHODS

2.1 | The PID test

The IEC 62804-1 test procedure was followed which prescribes application of a bias voltage from an external power source between the grounded module frame and the solar cells through the shorted two connectors from the junction box. The commercial modules we investigate in this study are frameless; therefore, they were supported with metal bars which were then connected to the power source with metal clamps (Figure 1). A voltage of -1000 V was applied for 48 h in a climate chamber at 85°C and 85% relative humidity (RH). I-V measurements were conducted, and EL images were taken both before and after the PID test. Another commercial module from the same production batch was also tested under damp heat conditions (85°C and 85% RH) without electrical bias.

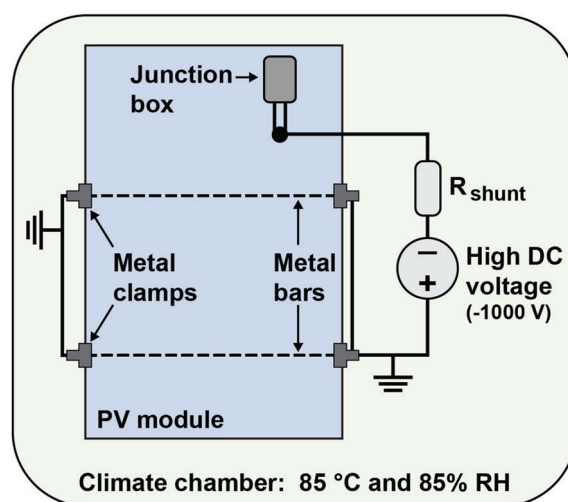


FIGURE 1 Schematic of the potential induced degradation test setup. The test was conducted on a frameless glass/glass commercial copper-(indium-gallium)-diselenide photovoltaic (PV) module [Colour figure can be viewed at wileyonlinelibrary.com]

2.2 | Coring and unpackaging

Figure 2 summarises the consecutive steps of coring and unpackaging. Based on the EL image taken after the PID test, areas of interest for post-mortem analysis were selected. A coring method was custom developed for sample extraction from the defined areas.^{18,19} A drilling machine with a hollow diamond drill put together with a water-cooling system was used for this application. The diameter of the drill for this study was chosen to be 3.5 cm, which yielded round samples with a diameter of 3.1 cm. The drilling was applied to the back of the module, which was placed in a tray with a plank support underneath. Coring was followed by unpackaging, where mechanical force was applied at an elevated temperature to separate the front glass from the encapsulant and then to peel off the encapsulant.

2.3 | Sample analysis

Figure 3 displays the cell fabrication on the extracted samples for investigation of electrical properties. Some active material loss can occur due to imperfect unpackaging, shown by blue crosses, where TCO/CdS/CIGS layers were removed during peeling of the encapsulant. The samples consisting of interconnected cells were prepared by scribing a defined area (blue rectangle) on the remaining active material and then by putting silver (Ag) contacts on the adjacent cells. The active material remaining outside of the new cells was removed to eliminate any contribution or leakage of current. I–V measurements were conducted at room temperature under 1000 W/m² simulated AM1.5G illumination using a Xenon lamp in a Neonsee solar simulator.

GreatEyes LumiSolarcell setup was used for PL imaging with a silicon charged-coupled device (CCD) camera. The samples were illuminated with two red light emitting diode (LED) lamps that have a peak emission at 660 nm. All images displayed in this paper were taken with a lens aperture of f/2.8 with integration time of 20 s. A black paper mask was used to cover the glass exposed from the scribes of the cored edge, which can saturate the luminescence image. ILIT measurements were performed using a setup by InfraTec with an ImagerR 8300 infrared camera. Two infrared LED lamps, with a peak emission wavelength at ~860 nm, were used to illuminate the samples. All reported ILIT images were taken with a 15- μ m lens, at a 5-Hz excitation frequency with integration time of 40 s. A GDA650-system built

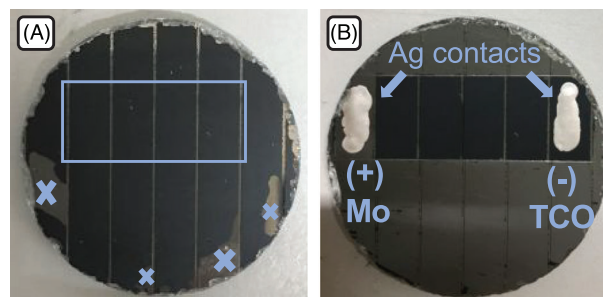


FIGURE 3 (A) Sample extracted from the photovoltaic module by coring. The rectangle shows the area defined for cell fabrication, whereas blue crosses show the areas where active material was lost during unpackaging. (B) Four-interconnected-cell fabricated on the samples for post-mortem analysis. Ag paint was used to make contacts for current–voltage measurements [Colour figure can be viewed at wileyonlinelibrary.com]

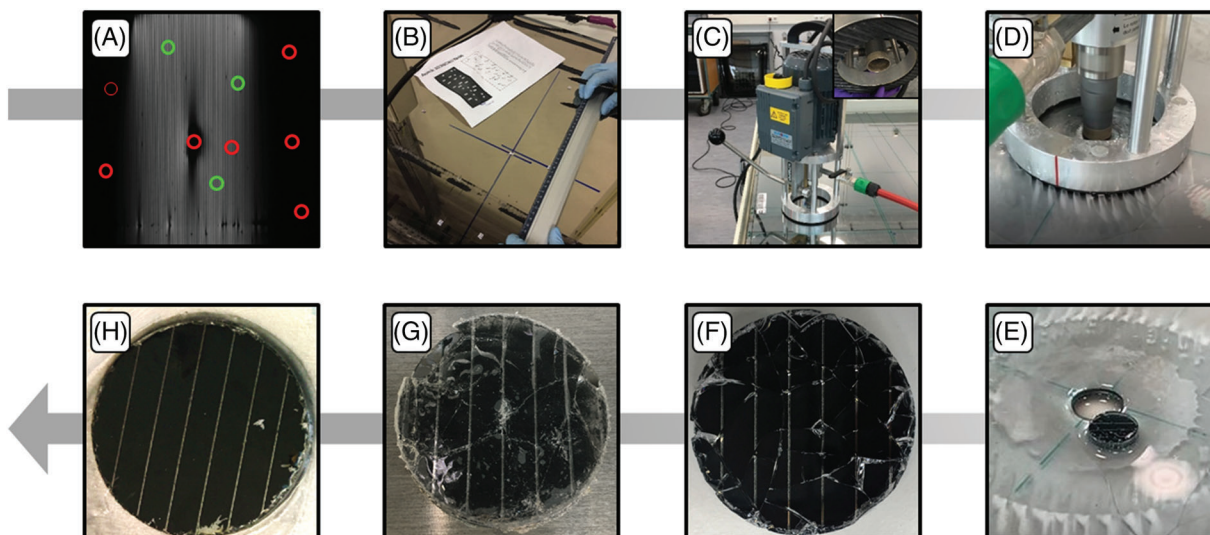


FIGURE 2 Intermediate steps of coring and unpackaging: (A) defining areas of interest for post-mortem analysis based on the electroluminescence image taken after the potential induced degradation test, (B) marking of areas on the commercial photovoltaic module, (C, D) hollow diamond drill used on the module, (E) extracted sample, and (F, G) zoom on packaged samples, which undergo cover glass and encapsulant removal to obtain (H) sample with the active layers accessible for measurements [Colour figure can be viewed at wileyonlinelibrary.com]

by Spectra Analytik was used to measure GD-OES depth profiles. An argon plasma was used for sputtering. The photons emitted were detected by a CCD array. The equipment includes a Grimm-type glow discharge source with an anode of 2.5-mm diameter and a non-conducting cathode plate.

3 | RESULTS AND DISCUSSIONS

3.1 | Post-mortem analysis of the module

Figure 4 shows the I–V curves of the field module measured before and after the PID tests conducted in a climate chamber at 85°C and 85% RH, with a bias of –1000 V for 48 h. Table 1 summarises the change in electrical parameters upon PID stressing. The power has dropped by 50%. The power drop was caused by V_{oc} and FF losses, which are 27% and 28%, respectively. On the contrary, the I_{sc} loss was only 4%. This is consistent with most of the literature on PID degradation of CIGS, where power losses are also related to drastic losses of V_{oc} and FF with no significant change in I_{sc} and R_{sh} . However, there have been studies in literature that reported negative effects on all I–V parameters, observing loss in I_{sc} and shunting.^{5,12,20,21} Table 1 also shows the changes in electrical properties for a module that was tested only in damp heat (DH) conditions without any bias application.

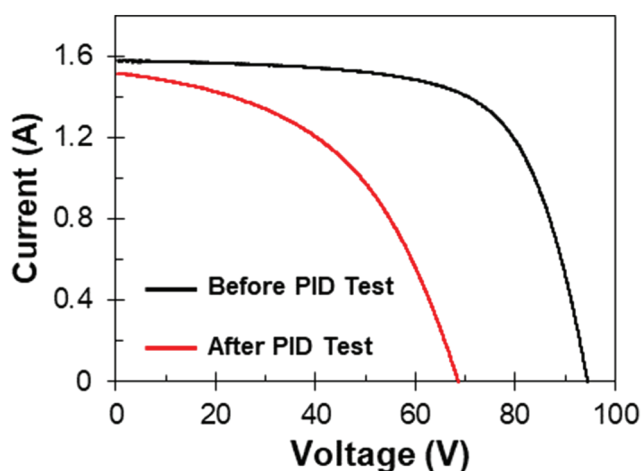


FIGURE 4 Current–voltage curves of the module before and after the potential induced degradation (PID) test (bias applied: –1000 V for 48 h, in a climate chamber at 85°C and 85% relative humidity) [Colour figure can be viewed at [wileyonlinelibrary.com](#)]

TABLE 1 Change of electrical properties of the module after the accelerated lifetime tests

	ΔP (%)	ΔV_{oc} (%)	ΔI_{sc} (%)	ΔFF (%)
Module (PID)	–50	–27	–4	–28
Module (DH)	7	0	1	6

Note: Potential induced degradation (PID) test: –1000 V at 85°C and 85% relative humidity, 48 h; damp heat (DH) test: 85°C and 85% relative humidity, 48 h.

There was no power degradation; on the contrary, a slight increase in module performance was noted. A possible explanation is the effect of thermal annealing during the heat exposure.²² Hence, the power losses in PID-tested module can be attributed to the additional bias application during the test.

The EL images of the field module taken before and after the PID tests are shown in Figure 5. Based on the EL image taken after the PID test, we made two observations:

1. Darkening at the module edges indicating degradation of the edge cells and
2. Formation of shunts along a horizontal line.

The areas closer to the edge are nonluminescent and appear darker compared with the centre of the module, which indicates degradation of the edge cells. This is because the potential distribution upon PID stressing is non-uniform across the module and the built-up potential difference between the cells versus the grounding is higher closer to the edges, leading to an increased PID effect. Due to relatively high glass surface conductivity under damp conditions, the potential applied to the module via the clamps and the support is spread over the outside of module, and it is similar around the perimeter in the edges and can go outside-in from the entire perimeter. Inversely, the solar cells in the central part of the module are still luminescent. These findings, along with the electrical measurements, suggest that the central (luminescent) part of the module is still active and generates current, but the edge cells have deteriorated, generating little power and causing series resistance.

On the other hand, the formation of shunts in the centre of the module was also clearly visible in the EL image, which was not present before the PID test. These shunts are also worth investigating as they

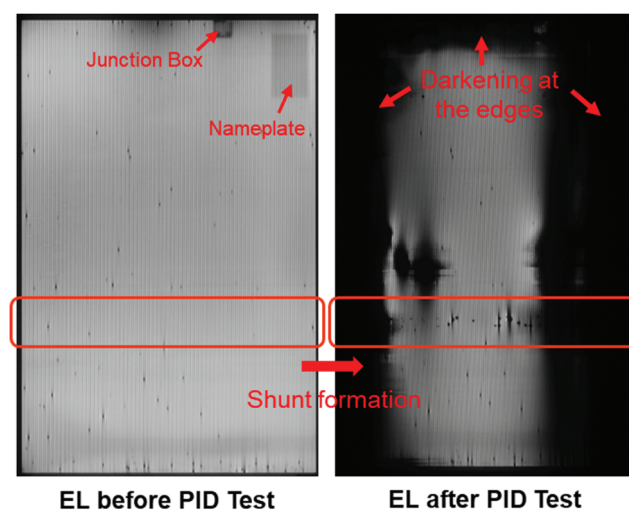


FIGURE 5 Electroluminescence (EL) images of a commercial frameless copper-(indium-gallium)-diselenide photovoltaic module taken before and after the potential induced degradation (PID) test (bias applied: –1000 V for 48 h, in a climate chamber of 85°C and 85% relative humidity) [Colour figure can be viewed at [wileyonlinelibrary.com](#)]

may reveal (other) degradation mechanisms and contribute to the performance losses.

After the macroscopic investigations on the field module were finalised, post-mortem analysis at the microscale was conducted with the samples that were extracted from the module by coring. Samples were selected from the areas of interest including the degraded (dark) areas and areas with shunts. The samples from each area are discussed separately in Sections 3.2 and 3.3.

3.2 | Post-mortem analysis of the extracted samples from the dark area

The samples were labelled and numbered as Dark and Reference representing degraded and nondegraded areas of the module, respectively. In total, three Reference and five Dark samples were investigated. Figure 6 exhibits the samples with their locations on the module, together with their electrical properties, and PL and ILIT images.

The PL imaging of the samples was performed together in pairs to enable a quantitative comparison between the samples. Consistent with the module's EL image before coring, the Reference samples have higher PL intensity and appear uniformly bright compared with the Dark samples that apparently exhibit less radiative recombination. For the Dark samples, it is important to add that the luminescence was uniform across the interconnected cells; a local shunt in the samples was not observed. This was also confirmed by ILIT images where the temperature variance was uniform across all cells and no local hot-spots were detected.

One interesting observation was made for sample Dark 8 which appeared dark in the EL image of the module but was brighter in the PL images compared with the other Dark samples. One possible explanation can be that PID might occur locally or degradation of the adjacent cells of the module may happen gradually. This can lead to

varying EL responses of the adjacent cells, and the low EL of the inactive cells might dominate the EL image of the whole module.

The current density - voltage (J-V) curves of all samples are shown in Figure 7. Reference samples have V_{oc} around 0.64 V with FF values over 65% and efficiencies over 12%, which match with the module's electrical performance prior to PID test implying that the coring and unpackaging processes do not harm the electrical properties of the solar cells. For the Dark samples which were extracted from degraded areas, a significant drop can be observed for V_{oc} and FF. V_{oc} decreases to values less than half of the reference samples, with efficiencies dropping below 3%. On the contrary, J_{sc} values are similar for all samples. The degraded samples still show a diode behaviour, and the flattening of the curves at further negative voltages

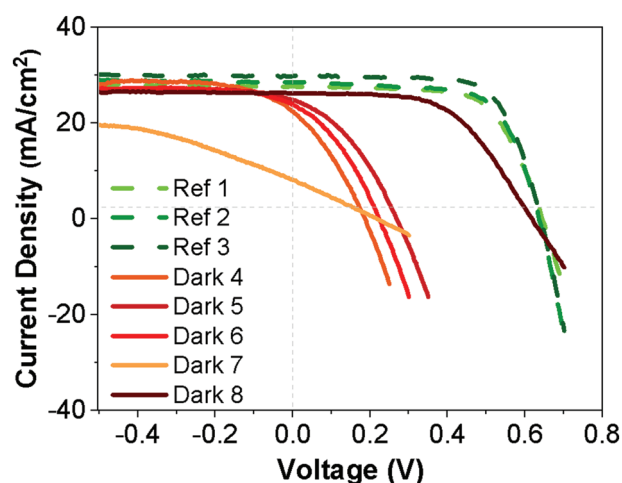


FIGURE 7 J-V curves of all samples that were extracted from both degraded (reference) and nondegraded (dark) areas. The curves are reported as voltage per cell versus short current density for comparison, as the number of interconnected cells and the cell area vary from sample to sample [Colour figure can be viewed at wileyonlinelibrary.com]

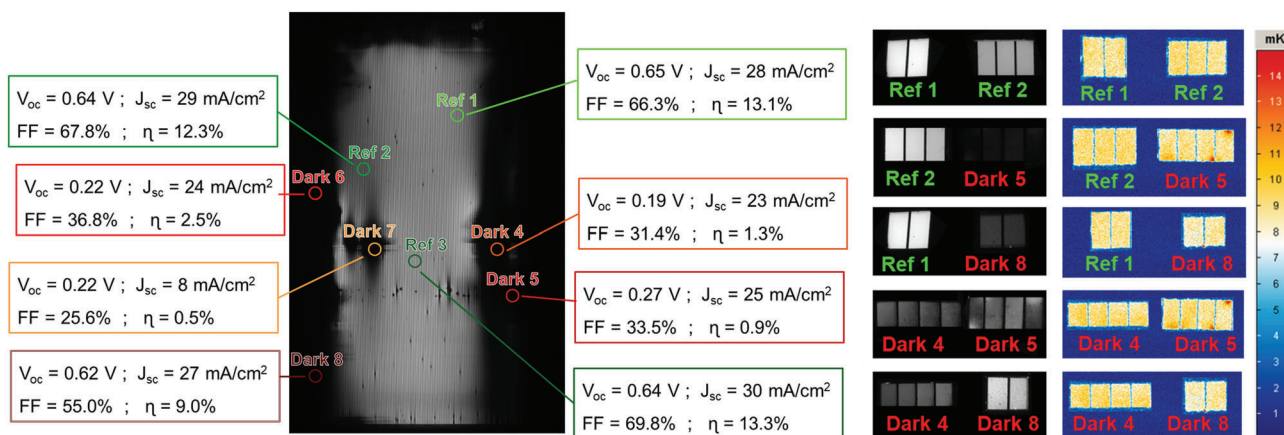


FIGURE 6 (left) Representations of all analysed samples with their locations on the copper-(indium-gallium)-diselenide photovoltaic module. The electrical parameters including V_{oc} , J_{sc} , FF, and efficiencies are reported. (right) Photoluminescence and illuminated lock-in thermography images are displayed in sets of combinations [Colour figure can be viewed at wileyonlinelibrary.com]

indicates similar R_{sh} values. However, Dark 7 stands as an exception compared with other samples. It acts as a (poor) resistor and has a high R_{sh} despite having the same degree of V_{oc} loss. Dark 8, which was aforementioned to have brighter PL intensity, had a smaller V_{oc} drop compared with other Dark samples.

We have performed GD-OES on selected samples to investigate if and at which layers sodium accumulated and whether we see a correlation between the degradation of electrical properties and the difference in sodium content. Figure 8 shows the sodium depth profiles, where the boundaries of the layers were defined based on the profiles of Zn, Cd, Ga, In, and Mo. A qualitative comparison in sodium intensities between the samples provides valuable information. Sodium profiles of the Reference and Dark samples show a notable increase in sodium content in the absorber layer only for samples that were extracted from the degraded area. These samples had less than half the V_{oc} values of the reference sample. Dark 8, which had a smaller V_{oc} drop compared with Dark 4 and Dark 5, also has a higher sodium content in its absorber layer, but the increase is much less significant. It is difficult to determine the precise location of sodium accumulation with GD-OES because the CdS layer is thin and merges into the CIGS absorber layer. On the other hand, no trace of sodium was found in the ZnO layers of all samples. Here, we would also like to note that secondary ion mass spectroscopy (SIMS) analysis on a similar PV module from the same production batch indicated that PID did not cause detectable changes in the concentration profiles of elements other than sodium such as Cr, Cu, and Mn.²³

Upon PID stressing, sodium is believed to be driven by a combination of drift and diffusion. The electrical bias promotes sodium drift from the glass sheets to the solar cell stack, and sodium migration to the adjacent layers follows a classical diffusion behaviour caused by concentration differences rather than an electric field.^{10,11,15} Inconsistent results have been reported in literature for the migration behaviour of sodium, which has led to varying degradation mechanisms proposed. Such contrasting observations can be related to different testing setups or PV devices with different materials or cell designs. There are two main scenarios for sodium migration in CIGS PV modules: either sodium migrates from the substrate glass and accumulates in the absorber layer especially close to CIGS/CdS interface or sodium migrates to the TCO layer from the cover glass.^{5,6,10} Our GD-OES measurements indicated that sodium accumulated in the upper region of the absorber layer, and it was not detected in the ZnO. We can therefore assume that in our study, sodium migration occurred from the substrate glass to the upper region of the absorber layer close to the interface (Figure 9). In correspondence to I-V measurements, the samples with higher sodium content also had significantly lower V_{oc} and FF values. Similar observations were reported in literature; degradation mechanisms behind PID failure were attributed to interstitial defects caused by sodium in both absorber layer and the CdS buffer layer resulting in lower doping density and minority lifetime, lowering the V_{oc} , and eventually damaging the p-n junction.^{10,11,17} As the sodium migration is from the substrate glass in our study, one way to resolve this could be to add a diffusion barrier layer between the glass substrate and the Mo layer. This issue and its possible mitigation

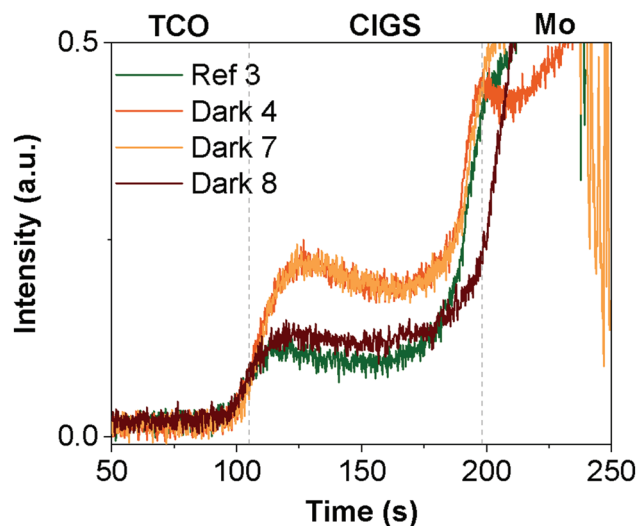


FIGURE 8 Glow discharge optical emission spectroscopy measurements performed for selected samples demonstrate sodium depth profile within the boundaries of the copper-(indium-gallium)-diselenide (CIGS) solar cell stack [Colour figure can be viewed at wileyonlinelibrary.com]

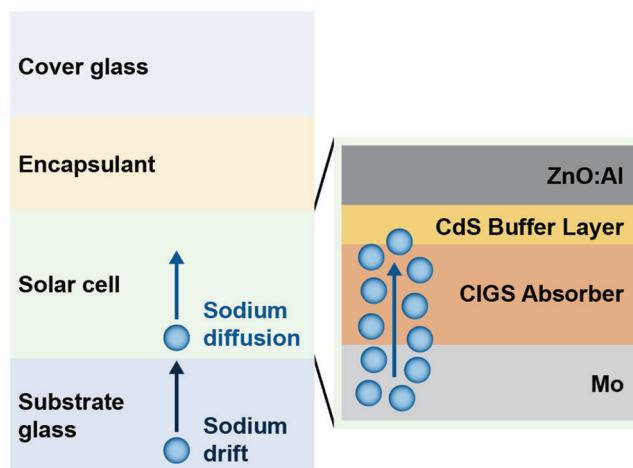


FIGURE 9 Sodium migration during potential induced degradation test: Sodium initially drifts from the glass substrate to the molybdenum back contact and then diffuses into the solar cell layers accumulating at the upper region of the copper-(indium-gallium)-diselenide (CIGS) absorber layer [Colour figure can be viewed at wileyonlinelibrary.com]

routes are discussed in more detail in our recently published CIGS PID review paper.¹²

3.3 | Post-mortem analysis of the extracted samples from the area with shunts

In addition to samples that were extracted from the degraded area of the module, we also investigated a sample from the area with local shunts formed after the PID test. Figure 10 shows where the sample

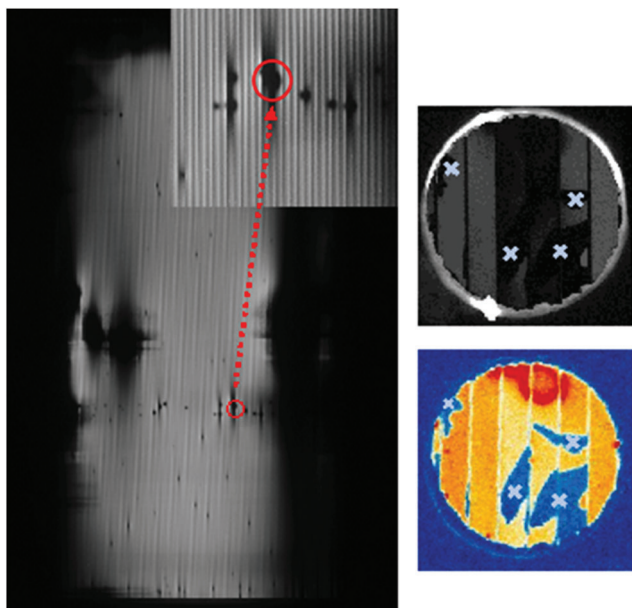


FIGURE 10 Photoluminescence and illuminated lock-in thermography images (right) of a sample extracted from an area with shunts. The location of the sample on the module is shown on the electroluminescence image [Colour figure can be viewed at wileyonlinelibrary.com]

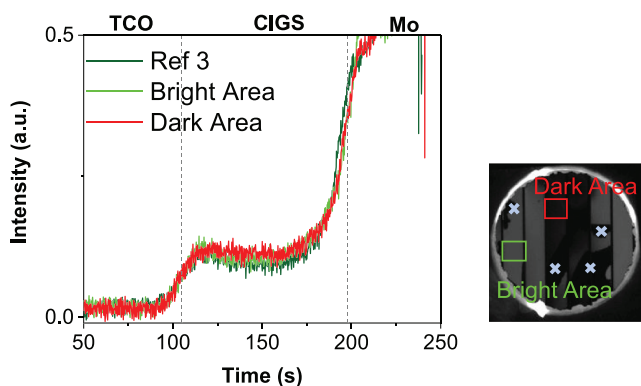


FIGURE 11 Sodium profile of a sample with a local shunt. The inset photoluminescence image displays the locations where glow discharge optical emission spectroscopy was performed. CIGS, copper-(indium-gallium)-diselenide [Colour figure can be viewed at wileyonlinelibrary.com]

was extracted from and the ILIT and PL images of the extracted sample. The PL image demonstrates that active cells have a high PL intensity, whereas the two middle cells with the shunt appear dark. A hotspot spread to four adjacent interconnected cells can also be observed in the ILIT image. Unfortunately, at this stage, we could not assess the impact on the power degradation because I–V measurements were not possible. However, we believe that their impact on the overall power degradation of the module is likely a lot smaller in comparison with the large degraded edge areas. Incidentally, brand new CIGS modules can display several such shunts in EL while matching the nameplate specifications.

We further investigated whether the formation of shunts after the PID test was also related to sodium migration by carrying out a GD-OES measurement. According to the PL map of the sample, two areas were defined for the measurement, namely, Bright Area (green box) and Dark Area (red box), corresponding to the active part and the shunt on the sample (Figure 11). The sodium profile of these regions together with that of a reference sample are displayed in Figure 11. No change in sodium content was observed for either area including the shunted region. We therefore cannot associate the formation of shunts within this area with sodium migration induced by the PID test. However, more statistics is required for a conclusive statement on this matter. We also suggest a study based on EL images of the whole module taken at different intervals during the PID test to further investigate the initial formation and the propagation of shunts.

4 | CONCLUSIONS

We examined a commercial CIGS PV module that was PID tested according to IEC 62804-1 standards (bias application of -1000 V at 85°C and 85% RH for 48 h). An EL image taken after the PID test allowed two main observations: (1) darkening at the module edges indicating degradation of the edge cells and (2) formation of local shunts along a horizontal line. A custom-developed method, *coring*, was then applied to extract small representative samples out of selected areas, which allows us to carry out an in-depth microscopic investigation on a full-size module using a set of laboratory-based techniques. A comparative analysis between the samples after the PID test shows that there are strong correlations between the degraded samples' PL intensities, V_{oc} values, and the sodium content within the solar cell. Samples with lower V_{oc} values are shown to have lower PL intensity and a higher sodium content in the CIGS absorber layer according to the GD-OES measurements. No trace of sodium was detected in the ZnO layer, which indicates that sodium migration occurs from the substrate glass to the solar cell. Sodium accumulation in the absorber layer degrades the electrical properties of the layers. Although more work is needed to fully understand the mechanisms at play, the present results connect earlier research on module PID to cell/mini-module PID, confirming that the phenomena observed on small samples also occur at the module level. This was made possible by *coring*, as this technique allowed us to conduct an in-depth post-mortem microscopic analysis on a field module.

ACKNOWLEDGMENTS

We would like to acknowledge the Early Research Program 'Sustainability & Reliability for solar and other (opto-)electronic thin-film devices' (STAR) from TNO for funding.

DATA AVAILABILITY STATEMENT

The data that support the findings will be available in TNO Database at <https://www.tno.nl/nl/> following an embargo from the date of publication to allow for commercialization of research findings.

ORCID

Pelin Yilmaz  <https://orcid.org/0000-0003-2696-0256>

REFERENCES

- Jordan DC, Silverman TJ, Wohlgemuth JH, Kurtz SR, VanSant KR. Photovoltaic failure and degradation modes. *Prog Photovolt*. 2017; 25(4):318-326.
- Theelen M, Daume F. Stability of Cu (In,Ga)Se₂ solar cells: a literature review. *Solar Energy*. 2016;133:586-627.
- Luo W, Khoo YS, Hacke P, et al. Potential-induced degradation in photovoltaic modules: a critical review. *Energ Environ Sci*. 2017;10(1): 43-68.
- Voswinckel S, Mikolajick T, Wesselak V. Influence of the active leakage current pathway on the potential induced degradation of CIGS thin film solar modules. *Solar Energy*. 2020;197:455-461.
- Fjällstrom V, Salomé PMP, Hultqvist A, et al. Potential-induced degradation of CuIn_{1-x}Ga_xSe₂. *IEEE J Photovolt*. 2013;3:1090-1094.
- Yamaguchi S, Jonai S, Hara K, et al. Potential-induced degradation of Cu (In,Ga)Se₂ photovoltaic modules. *Jpn J Appl Phys*. 2015;54(8): 697-708.
- Naumann V, Lausch D, Hähnel A, et al. Explanation of potential-induced degradation of the shunting type by Na decoration of stacking faults in Si solar cells. *Solar Energy Mater Solar Cell*. 2014;120: 383-389.
- Swanson R, Cudzinovic M, DeCeuster D, Desai V, Jürgens J, Kaminar N, Mulligan W, Rodrigues-Barbarosa L, Rose D, Smith D, Terao A, Wilson K. The Surface Polarization Effect in High-Efficiency Silicon Solar Cells. *Proceedings of 15th International Photovoltaic Solar Energy Conference and Exhibition, 2005*; 410.
- Fjällstrom V, Szaniawski P, Vermang B, et al. Recovery after potential-induced degradation of CuIn_(1-x)Ga_xSe₂ solar cells with CdS and Zn(O,S) buffer layers. *IEEE J Photovolt*. 2015;5(2):664-669.
- Muzzillo CP, Glynn S, Hacke P, et al. Potential-induced degradation of Cu (In,Ga)Se₂ solar cells: alkali metal drift and diffusion effects. *IEEE J Photovolt*. 2018;8(5):1337-1342.
- Xiao C, Jiang C, Harvey SP, Mansfield L, et al. In-Situ Microscopy Characterization of Cu (In,Ga)Se₂ Potential-Induced Degradation. *Proceedings of 46th IEEE Photovoltaic Specialists Conference, 2019*; 2342-2345.
- Yilmaz P, Schmitz J, Theelen M. Potential induced degradation of CIGS PV systems: a literature review. *Renew Sustain Energy Rev*. 2022;154:111819.
- Boulhidja S, Mellit A, Voswinckel S, et al. Experimental evidence of PID effect on CIGS photovoltaic modules. *Energies*. 2020;13(3):537.
- Alonso-Garcia MC, Hacke P, Glynn S, Muzzillo CP, Mansfield LM. Analysis of potential-induced degradation in Cu (In,Ga)Se₂ samples. *IEEE J Photovolt*. 2019;9(1):331-338.
- Harvey SP, Guthrey H, Muzzillo CP, et al. Investigating PID shunting in polycrystalline CIGS devices via multi-scale, multi-technique characterization. *IEEE J Photovolt*. 2019;9(2):559-564.
- Muzzillo CP, Glynn S, Hacke P, et al. Potential-induced degradation depends on leakage current and light/electrical bias in Cu (In,Ga)Se₂ devices. *IEEE J Photovolt*. 2019;9(6):1852-1856.
- Salomon O, Hempel W, Kiowski O, et al. Influence of molybdenum back contact on the PID effect for Cu (In,Ga)Se₂ solar cells. *Coatings*. 2019;9(12):794.
- Moutinho HR, Johnston S, To B, et al. Development of coring procedures applied to Si, CdTe, and CIGS solar panels. *Solar Energy*. 2018; 161:235-241.
- Moutinho H. R, To B, Jiang C-S, Xiao C, Muzzillo C. P, Hacke P, Moseley J, Tynan J, Dhery N. G, Mansfield L, Al-Jassim M. M, Johnston S. Artifact-free coring procedures for removing samples from photovoltaic modules for microscopic analysis. *Proceedings of IEEE 7th World Conference on Photovoltaic Energy Conversion (WCPEC) (A Joint Conference of 45th IEEE PVSC, 28th PVSEC & 34th EU PVSEC), 2018*; 1313-1317.
- Boulhidja S, Mellit A, Voswinckel S. Potential-induced degradation test on CIGS photovoltaic modules. *Proceedings of 5th International Conference on Electrical Engineering, 2017*;1-4.
- Hacke P, Kempe M, Wohlgemuth J, Li J, Shen YC. Workshop on crystalline silicon solar cells and modules: materials and processes; 2016.
- Flammini G, Debernadi N, Le Ster M, Dunne B, Bosman J, Theelen M. The influence of heating time and temperature on the properties of CIGSe solar cells. *Int J Photoenergy*. 2016;2016:1-7.
- Yilmaz et al. (in preparation)

How to cite this article: Yilmaz P, Aninat R, Cruz GO, Weber T, Schmitz J, Theelen M. Post-mortem analysis of a commercial Copper Indium Gallium Diselenide (CIGS) photovoltaic module after potential induced degradation. *Prog Photovolt Res Appl*. 2022;1-8. doi:10.1002/pip.3538